Effect of NBI on thermal quench dynamics in TCV disruptions

L. Ekman[1*], M. Hoppe[1], L. Votta[1], J. Decker[2], G. Partesotti[2], M. Pedrini[2], U. Sheikh[2], B. Vincent[2], the TCV Team[†] and the EUROfusion Tokamak Exploitation Team[‡]

[1] *Department of Electromagnetics and Plasma Physics, KTH Royal Institute of Technology, SE-10044 Stockholm, Sweden,*

[2] *École Polytechnique Fédérale de Lausanne, Swiss Plasma Center, CH-1015 Lausanne, Switzerland,*

[†] *see author list of Christian Theiler* et al *2026 Nucl. Fusion in press,*

[‡] *see the author list of N. Vianello* et al *2026 Nucl. Fusion in press.*

Introduction

Finding effective methods to mitigate runaway electron generation is a critical challenge for the development of reactor-scale tokamaks, where uncontrolled runaway beams could cause severe damage to plasma-facing components [1]. One possible mitigation mechanism is to slow down the thermal quench using auxiliary heating, thereby reducing the formation of hot-tail runaway electrons [2].

In this work, a neutral beam injection (NBI) heating model is implemented in the disruption simulation framework DREAM [3]. This model is used to investigate the effect of NBI on thermal quench dynamics by constraining free parameters with bayesian inference, and to assess the resulting hot-tail runaway electron generation. The study is motivated by measurements of the electron temperature from the Tokamak á Configuration Variable (TCV), shown in Fig. 1. There, discharges with NBI heating of 500 kW and 1000 kW are compared with a reference discharge without NBI, showing a delayed thermal quench with increasing NBI.

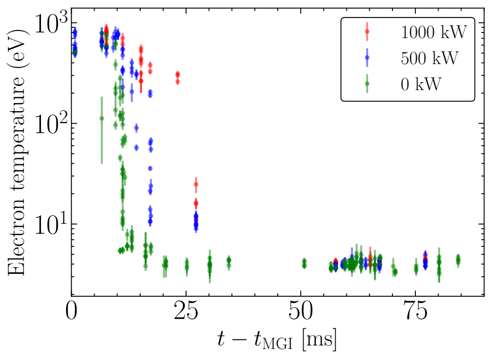

Figure 1: Electron temperature measurements from Thomson scattering channels for each NBI power level.

Simulation and experimental setup

In this work, the NBI model accounts for the spatial distribution of beam-particle deposition as the injected neutrals propagate through the plasma. The deposition profile is modelled as

$$H(r) = \frac{1}{V'} \int \mathrm{d}\theta \int \mathrm{d}\phi \ \mathscr{J} \ \frac{j_{\mathrm{B}}(r_{\mathrm{B}}, \theta_{\mathrm{B}})}{I_{\mathrm{B}}} \frac{1}{\lambda(s_{\mathrm{B}})} D(s_{\mathrm{B}}), \tag{1}$$

where j_B/I_B is the normalized beam current density profile (particle flux equivalent), (r_B, θ_B) parametrize the beam cross-section, and s_B is the coordinate along the beam axis. The quantities $\mathscr{J}$ and V' are the plasma configuration-space Jacobian and the flux-surface volume element, respectively. The survival probability of the beam particles is denoted by $D(s_B)$, while $\lambda(s_B)$ is the local mean free path, including charge exchange with ions and electron-impact ionization.

The deposition profile is multiplied by the injected NBI power and added as a heating source in the DREAM power-balance equations for ions and electrons [3]. The beam geometry is defined by a starting point and a direction vector, and to evaluate the particle deposition efficiently, the full beam is divided into a set of pencil beams. For each grid point, a computationally efficient line-search is used to identify the closest intersection between the pencil beam and the corresponding flux surface. The total deposition profile is then obtained by summing the contributions from all pencil beams.

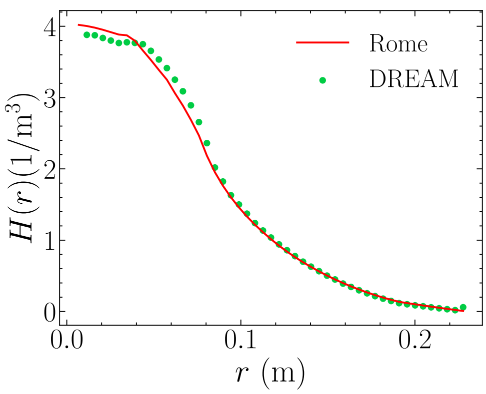

Figure 2: Deposition profiles in the DREAM and Rome models.

The NBI deposition model is validated against an analytical model of Rome et al. [4], using circular flux surfaces and a parabolic density profile, as shown in Fig. 2. The discrepancies are mainly due to the differences in the mean free path: in the Rome model it depends only on the plasma density, while in DREAM it is computed from ADAS ionization rates and therefore depends on the local plasma conditions.

DREAM simulations are initialized from TCV discharges #86634, #86645, and #86654, corresponding to 1000 kW, 500 kW, and a no-NBI reference case, respectively. Comparison with experimental line-integrated density data showed that the neon injection should be modelled with a finite injection time, and radiation and AXUV measurements further indicated that the thermal-quench dynamics require at least three distinct phases of radial heat diffusion. The neon-injection time and the three heat diffusion coefficients are therefore constrained using bayesian inference [5], with an distance function based on experimental data from electron temperature, radiated power, and line-integrated density.

Modeling results

The modeling results are presented in two parts. The first part discusses the bayesian inference results and examines how NBI modifies the thermal-quench dynamics. The second part focuses on hot-tail runaway generation, comparing the fluid and kinetic models in DREAM .

Bayesian inference of free parameters

Fig. 3 shows the optimal simulation according to the bayesian inference for #86634, #86645 and #86654, compared with the corresponding TCV measurements. Good agreement is obtained for all three discharges: the simulated temperature evolution agrees well with the electron temperature measured by Thomson scattering, and the main radiation features are captured, including the dominant peaks in #86634 (Fig. 3(b)), the peak and plateau in #86645 (Fig. 3(e)), and the smaller peak in #86654 (Fig. 3(h)). The line-integrated density agrees well during the initial rise, which is directly related to the assimilated neon. The later evolution may be influenced by transport and recycling processes not included in the model. Moreover, the inferred neon injection time similar for all cases, as expected, and is in the range of approximately 10 ms to 15 ms. In addition, the optimized heat-diffusion coefficients converge to values of order $1\,\mathrm{m^2\,s^{-1}}$ to $10\,\mathrm{m^2\,s^{-1}}$, corresponding to energy confinement times comparable to those during the TCV flat-top phase [6].

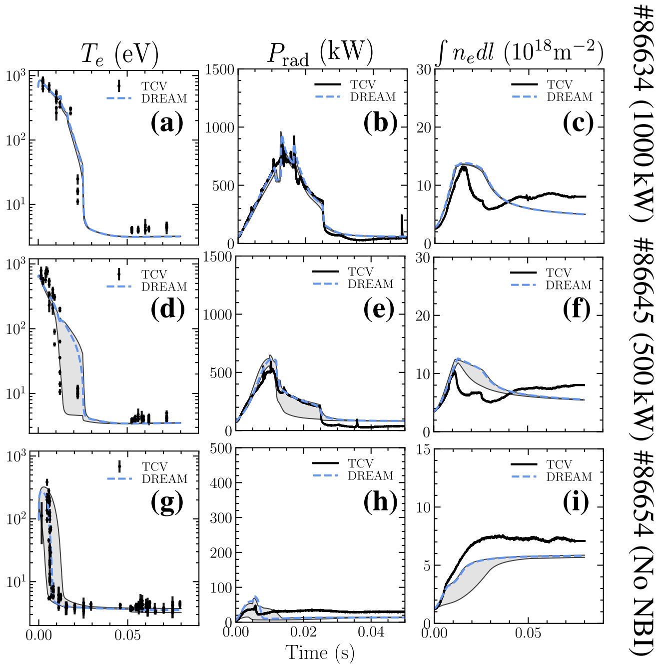

Figure 3: Simulations with the optimal set of free parameters from the Bayesian inference. Gray shaded regions indicate the variation obtained when the free parameters are varied within their estimated local uncertainty intervals around the optimum.

Fig. 4 shows that NBI mainly affects the power balance by depositing additional energy into both ions and electrons. This sustains higher temperatures during the disruption, leading to increased radiation while the beam is active and delaying the subsequent cooling. The higher temperature also maintains a higher conductivity, so the ohmic current and ohmic heating decay more slowly. Since part of the NBI power is deposited into ions, the ion–electron energy exchange also increases, transferring this energy to the electrons.

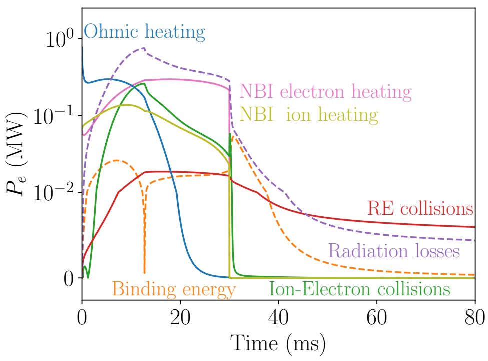

Figure 4: Electron power balance for discharge #86645, evaluated with the optimized free parameters held fixed and an NBI power of 1000 kW.

Hot-tail runaway electrons

The initial conditions from discharge #52717 are used to compare the fluid and kinetic hot-tail runaway-electron models in DREAM, both with 1000 kW NBI and without NBI. As shown in Fig. 5, the kinetic simulations reveal a delayed phase in which NBI can lead to an increased runaway-electron density. Although NBI initially reduces hot-tail generation, this leaves a larger fraction of the current to be carried ohmically. The resulting electric-field rise is delayed, but eventually becomes stronger than in the no-NBI case, yielding stronger overall runaway generation. This delayed effect is not captured by the fluid model, where the distribution function collapses earlier.

Conclusions

A neutral-beam-injection heating model has been implemented in DREAM and validated against the analytical model of Rome *et al* [4]. The model was applied to TCV disruptions with 500 kW and 1000 kW NBI, together with a no-NBI reference case. Using bayesian inference to constrain the neon injection time and heat-transport coefficients, the simulations reproduce the main experimental trends in temperature, radiation, and line-integrated density, as well as explainable optimal values for the inferred free parameters.

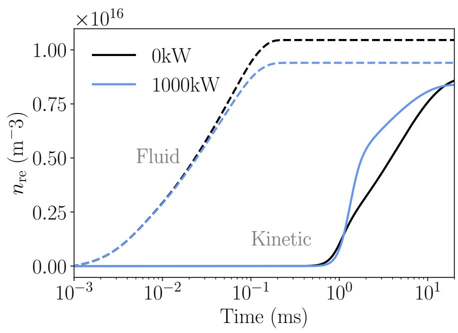

Figure 5: Hot-tail runaway electron density evolution for the fluid and kinetic models, comparing the 0 kW and 1000 kW NBI cases.

The results show that NBI can delay the thermal quench in TCV by sustaining higher plasma temperatures and modifying the power balance. However, the final runaway-electron density is only weakly affected in the studied cases. Kinetic simulations further indicate that although NBI initially suppresses hot-tail generation, the delayed electric-field evolution can later increase runaway production. Additional tests with ITER-like parameters showed no significant NBI effect, suggesting that the impact is likely limited in larger devices.

References

[1] S. Ratynskaia *et al.*, Plasma Physics and Controlled Fusion (2026).
[2] V. V. Plyusnin *et al.*, Proceedings of the 30th EPS Conference on Plasma Physics (2003).
[3] M. Hoppe *et al.*, Computer Physics Communications (2021).
[4] J. A. Rome *et al.*, Nuclear Fusion **14**, 2 (1974).
[5] A. E. Järvinen *et al.*, Journal of Plasma Physics **88**, 6 (2022).
[6] J. Decker *et al.*, Nuclear Fusion **64**, 10 (2024).

This work has been carried out within the framework of the EUROfusion Consortium, partially funded by the European Union via the Euratom Research and Training Programme (Grant Agreement No 101052200 — EUROfusion). The Swiss contribution to this work has been funded by the Swiss State Secretariat for Education, Research and Innovation (SERI). Views and opinions expressed are however those of the author(s) only and do not necessarily reflect those of the European Union, the European Commission or SERI. Neither the European Union nor the European Commission nor SERI can be held responsible for them.